Tribological behaviour of AISI 316L stainless steel for biomedical applications

M. Fellah*, M. Labaïz, O. Assala, A. Iost and Leila Dekhil

The aim of this research is to study the tribological behaviour of AISI 316L stainless steel for surgical implants (total hip prosthesis). The tribological behaviour is evaluated by wear tests, using tribometers ball on disc and sphere on plane. These tests consisted of measuring the weight loss and the friction coefficient of stainless steel (SS) AISI 316L. The oscillating friction and wear tests have been carried out in ambient air with an oscillating tribotester in accord with standards ISO 7148, ASTM G99-95a and ASTM G133-95 under different conditions of normal applied load (3, 6 and 10 N) and sliding speed (1, 15 and 25 mm s^{-1}). A ball of 100Cr 6, 10 mm in diameter, is used as counter pairs. These tribological results are compared with those carried out with a tribometer type pin on disc under different conditions of normal load applied P (19·43, 28 and 44 N) and sliding speed (600 and 1020 rev min^{-1}). The behaviour observed for both samples suggests that the wear and friction mechanism during the tests is the same, and to increase the resistance to wear and friction of biomedical SS AISI 316L alloy used in total hip prosthesis (femoral stems), surface coating and treatment are necessary.

Keywords: Tribological behaviour, Friction, Wear, Biomaterial, Prosthetic, Tribometer, SS AISI 316L

Introduction

Biomedical prosthetic devices are used in the human body to carry out functions that can no longer be performed by the original human parts. Metals are mainly used for orthopaedic purposes in humans, so their degradation by wear and corrosion must be negligible so that they can be used for various practical applications.[1] Among the various metallic materials that are used for orthopaedic devices, 316L stainless steel (SS) is one of the most commonly used. It is often used for temporary devices in orthopaedic surgery because of its low cost and acceptable biocompatibility.[2] However, under some conditions, this alloy suffers localised corrosion under some conditions and releases significant quantities of iron to neighbouring tissues, inducing fibrosis around the implant.[3–5] To overcome this problem, the prostheses should possess and also ensure high mechanical resistance. It should also have high corrosion resistance and the best possible adhesion to the tissue so that a stable biological bond with the bone is formed.[6–8]

Materials and method

Materials

SS AISI 316L is used in this study as a total hip prosthesis (femoral stem) (supplied by ENSAM Lille, France). The composition of the alloy is given in Table 2.

It is known that the fixation is greatly Correct dependent on good mechanical interlocking between the rough surface of the implant and tissue.[9] Therefore, the alloy surfaces were abraded with 600 grit abrasive paper and then polished with colloidal silica to a surface roughness R_a of ~0·025 μm. The samples were cleaned in an ultrasonic bath with acetone, ethanol and distilled water, respectively, for 10 min and then dried in hot air and saved in the desiccators for use in different characterisation tests.

Surface and microstructural analysis

The sample was polished with SiC paper and then 1 μm diamond paste, with the polished surface etched with an acidic etchant (1 part HF, 2 parts HNO_3 and 3 parts of H_2O). The microstructure (Fig. 4) was studied using optical microscopy (Leica DMLM). The chemical composition (Table 2) was acquired using a spectrometer (Spectrolab) and energy dispersive spectroscopy (Philips XL 30 ESEM-FEG and EDX IMIX-PTS). The phases (Fig. 8) present were identified by X-ray diffractometry (Intel CPS 120/Brucker AXS) using Cu K_α generated at 40 kV and 35 mA. Scanning electron microscopy (SEM) and energy dispersive X-ray analysis (EDX) were used to study the chemical composition of the SS AISI 316L (Fig. 7). The roughness (Fig. 6) of the SS in 3D was studied using Surface Data Veeco: Mag 5·0 X, Mode VSI. The SEM and EDX (Fig. 7) were used to study the chemical composition of the substrate.

Tribological study

In this work, pin on disc, ball on disc and sphere on plane tribological tests (Figs. 1–3) were carried out using

Surface Engineering and Tribology Group, Laboratory of Metallurgy and Engineering Materials, Badji Mokhtar Annaba- University, PO box 12, 23000, Algeria

*Corresponding author, email mamoun.fellah@yahoo.fr

Received 24 November 2012; accepted 1 April 2013
DOI 10.1179/1751584X13Y.0000000032

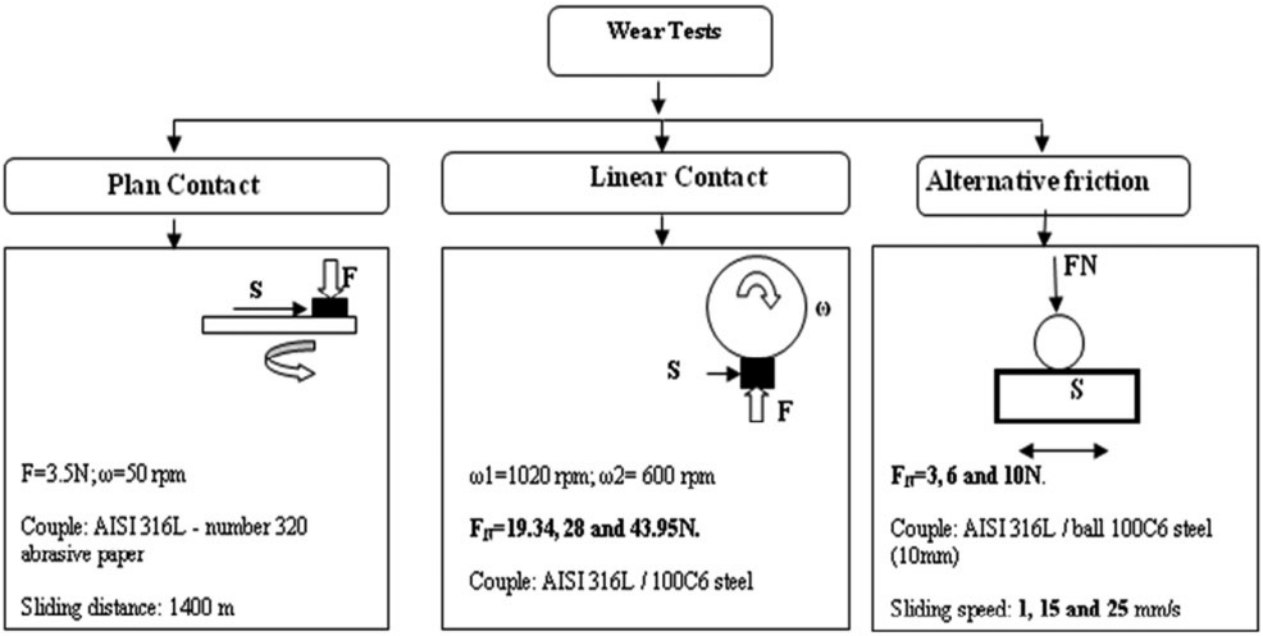

1 Conditions of wear tests

the following prosthetic materials: AISI 316L austenitic SS alloy against 100C6 and abrasive paper number 320 (Sic). Figure 1 shows a simplified scheme of the conditions of friction and wear tests.

Contact plan wear test

The contact pair, which studies the tribological pair, the sample [AISI 316L SS] and sandpaper (320 abrasive papers). The parameters for this test are applied load and rotational speed. The test time is kept constant, and the weight loss is the weight difference of the sample measured before and after the test with a microelectronic balance with an accuracy on the order 10^{-3} g. The samples were cleaned with acetone before being weighed; the surface roughness of the test sample is measured before and after the test. Absolute weight loss was determined by the following equation

$$\Delta P = P - P_i$$

where P_i is the weight measured after each time of wear, and P_o is the initial weight. The distance parcourue X (m) is determined as follows: $X = V/\tau$, with τ as sliding times, as the linear speed V is equal to the product of the angular velocity ω by the radius of sandpaper r

$$V = \omega r = \frac{2\pi n}{60r}; \quad X = \frac{\omega r}{\tau} = \frac{2\pi n r}{60\tau}$$

Figure 2 shows a simplified scheme of the contact plan wear test conducted in the Physical Metallurgy laboratory, Department of Metallurgy and Materials Engineering, Annaba University.

Friction behaviour

In this work, oscillating friction and wear tests have been carried out in ambient air with oscillating tribometer in accord with standards ISO 7148, ASTM G99-95a and ASTM G133-95 (Figs. 1–3) under different conditions of normal load (3, 6 and 10 N) and sliding speed (1, 15 and 25 mm s^{-1}). As counter pairs, a ball of 100Cr6 steel, 10 mm in diameter, was used as given in Table 2. A second tribological test is conducted with tribometer type pin on disc under different conditions of normal load P (19·43, 28 and 44 N) and sliding speed (600 and 1020 rev min^{-1}), to confirm the tribological results (Fig. 2*a*).

Table 1 Energy dispersive X-ray analysis of AISI 316L SS

Element	C	Cr	Ni	Mo	Mn	Si
at-%	0·016	21·18	10·24	2·03	1·60	0·33

Results and discussion

Surface and microstructural analysis

The SS sample was examined using EDX analysis. The spectra for the overall analyses are shown in Figs. 7 and 8. The EDX spectrum shows different peaks which correspond to the different elements contained in the substrate. The Fe peak is more pronounced than chromium, as expected in the EDX phases. Nickel, manganese, molybdenum and aluminium are also present (Table 2). The composition of the steel was in compliance with that of an AISI 316L SS.

Roughness analysis

The AISI 316l SS substrates are of biomedical interest. Therefore, they must meet biomedical ISO standards particularly at the surface of the material deposited on the articular surfaces of hip prostheses in which AISI 316l is the hip implant. The roughness of the SS AISI 316L was obtained (Table 3 and Figs. 5 and 6). It meets the biomedical standards of biomedicine, namely, roughness for metal parts as specified in ISO 7206-2:1996.[10]

Microhardness

Microhardness experiments were performed using a Zwick Roell Z 2·5 Micro Compression Tester type ZHU/Z2·5 equipped with a diamond indenter, at a room temperature of 22°C and laboratory atmosphere. Using the *P–h* (load–displacement) curves during

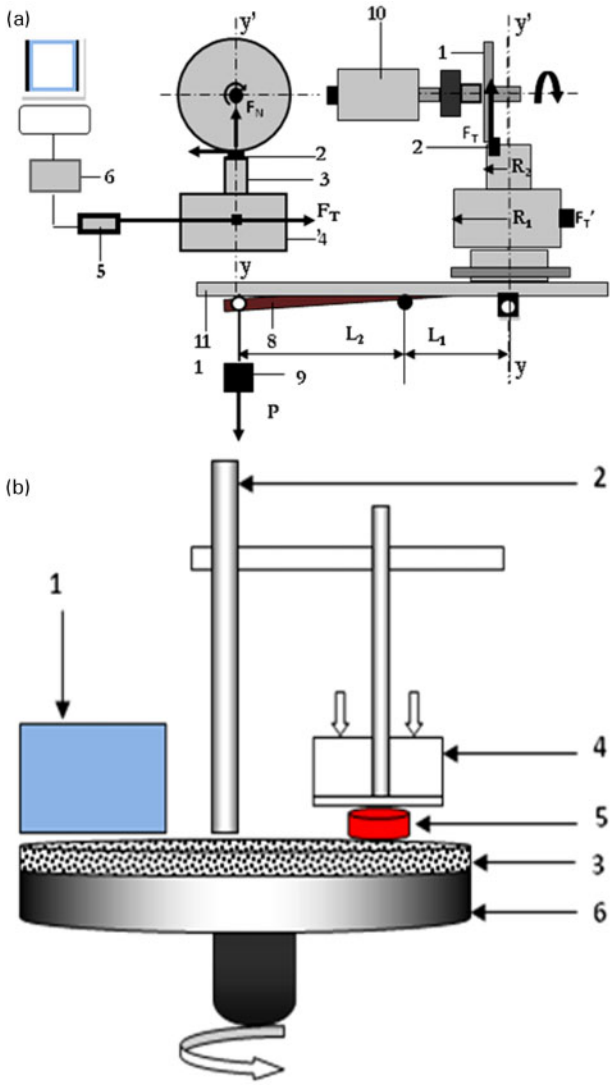

a linear contact: steel disc 100C6 treated (1), in contact of sample (2); (3) carry sample; swing of load (8) connected, on one side, with drum (4) and on other one with the weight (9); (6) interface; (7) computer; (10) motor; (11) table, sensor (5) to measure the tangential effort, connected (bound) with the drum; *b* scheme of contact geometry (plan contact): 1, speed regulator; 2, support; 3, rotating tray; 4, load applied; 5, sample; 6, retaining frame (friction pair used: AISI 316L sliding against number 320 abrasive paper; sliding distance, 1400 m)

2 Scheme of contact geometry

Microhardness experiments with a loading speed of 0·2 mm min^{-1} under a maximum load of 50 N, each test was conducted three times, and the average values were calculated automatically by MCT as the load and displacement. The experimental *P–h* curve of AISI 316L is shown in Figs 9–10. The hardness was measured as 315 ± 5 kgf mm^{-2}.

Tribological results

Plan contact

The weight loss (Fig. 11) of AISI 316L and ceramic samples, tested at 3·5 N load, is approximately proportional to the number of revolutions. Nevertheless, the wear was systematically greater to AISI 316L as expected. The behaviour observed for both samples suggests that the wear mechanism during the test is the same (abrasive wear). In the case of ceramic samples, the weight loss was ~15% of that observed for AISI 316L samples.

Linear contact

The evolution curves of friction coefficient versus time (Table 4 and Fig. 13) are almost the same from wholes in terms of load and speed. The analysis of these curves distinguishes several periods or successive regimes of friction and wear.

The first period, during which the friction coefficient increases rapidly, an accommodation, is the surface of the first body that is most ductile,[11] in this case, the steel. The relief is so attenuated; the roughness of the surface of the steel is reduced by plastic deformation.

The second period is characterised by a slight decrease in the friction coefficient. Probably, the third body on the track generated by frictional wear of the steel plays a role comparable to that of a solid lubricant.

The third period is defined by a significant increase in the friction coefficient. The third body is fragmented, oxidises and probably plays a role as abrasive, then the virtual stabilisation of the friction coefficient.

The fourth and final period is near stabilisation of the friction coefficient. The wear marks on 316L sample after wear test. (severe deformation and plastic flow) are presented in figure 12.

Alternative movement

It is important to know the wear and friction coefficient of ball 100C6 steel (Fig. 14) before studying the friction coefficient of studied materials.[12]

Influence of load applied (normal load)

The friction test results of AISI 316L SS at alternative movement versus 100C6 Ball are illustrated in Tables 5–7 and Figs. 15–20 respectively.

It is seen from Table 5 and Fig. 15 that the friction coefficient showed lower (min) values (approximately CF min.: 0·017, 0·069 and 0·103 at normal load 3, 6 and 10 N respectively) up to 200 distance (cycle) and then it increased to the average 0·508 value at 500 distance (cycle). This may be due to the formation of an oxide layer on the SS.

In Table 6 and Fig. 16, it is seen that the average friction coefficient was obtained as 0·74, 0·726 and 0·7 of the SS AISI 316l at normal load 3, 6 and 10 N respectively. It is also shown in Fig. 16 that the coefficient of friction displayed a lower value of 0·17, 0·124 and 0·263 up to 100 distance (cycle), and then it sharply increased to the average value of 0·74 until 2300 distance (cycle) distance.

It is seen that the average friction coefficient at different loads (3, 6 and 10 N) has the same values. The hertz pressure calculated is 690, 870 and 1031 MPa for loads 3, 6 and 10 N, respectively at alternative speed movement of 15 mm s^{-1}.

At a sliding speed of 25 mm s^{-1} as shown in Table 7 and Fig. 17, it is seen that the average value of friction coefficient was obtained at loads 3 and 6 N (0·71 and 0·75) of the SS AISI respectively. It is also obvious in Fig. 16 that the coefficient of friction displayed a lower value at 0·127, up to 50 distance (cycle), and then it sharply increased to the average value of 0·59 until 1400 distance (cycle).

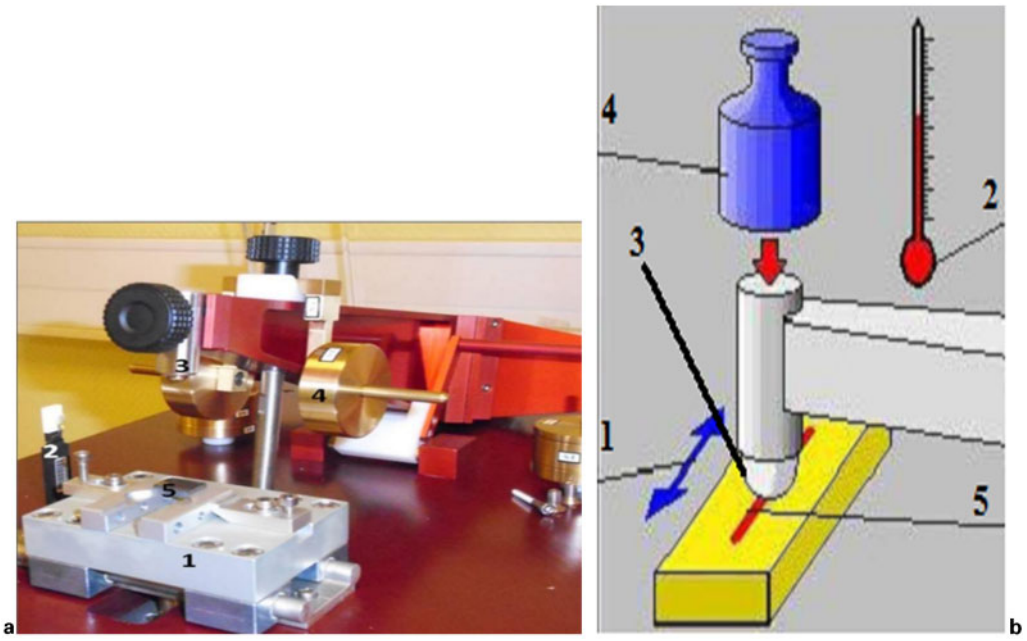

3 *a* photography and *b* scheme of contact geometry (alternative movement) and tribotester system at CER Arts & Métiers Paris Tech ENSAM Lille [1: table, carry sample on alternative movement (wear track radius=10 mm; 2: sensor to measure heat and humidity; 3: ball 100C6 steel; 4: load applied FN; 5: sample]

Influence of sliding speed

In Figs. 18–20, it is seen that the friction coefficient is the same value at sliding speeds of 15 and 25 mm s^{-1} under different normal loads of 3, 6 and 10 N. At 1 mm s^{-1}, it always has a lower value than those at 15 and 25 mm s^{-1}.

Wear

In the wear test, the volumetric wear rate (Table 8) was calculated using a mechanical profilometer as 53×10^{-3} mm^3 N^{-1} mm^{-1} for the SS. A 100C6 ball did the grinding from the sample surface, that is, abrasive wear occurred on the surface and this is illustrated in Figs. 21 and 22. Volumetric wears were determined as $7{\cdot}23 \times 10^{-3}$, $9{\cdot}56 \times 10^{-3}$ and $15{\cdot}05 \times 10^{-3}$ mm^3 N^{-1} mm^{-1} for the 1 mm s^{-1} sliding speed under loads of 3, 6 and 10 N respectively. Finally, the volumetric wears were the same for both sliding speeds of 15 and 25mm s^{-1} between $23{\cdot}67 \times 10^{-3}$ and 64×10^{-3} mm^3 N^{-1} mm^{-1}.

Friction versus wear

The strength of materials depends on three groups of factors in friction conditions.[13] Those factors are as follows:

(i) internal reasons determined by material properties;
(ii) friction type (slipping and rolling) and working conditions (relative movement speed, load, application type and temperature);
(iii) working environment and lubricants.

Conclusions

AISI 316L SSs predominate as materials for prosthetic devices because they are relatively inexpensive and formable by common techniques. Further, their mechanical properties are controllable over a wide range, providing optimum strength and ductility. However, SSs are the least corrosion resistant over the long term

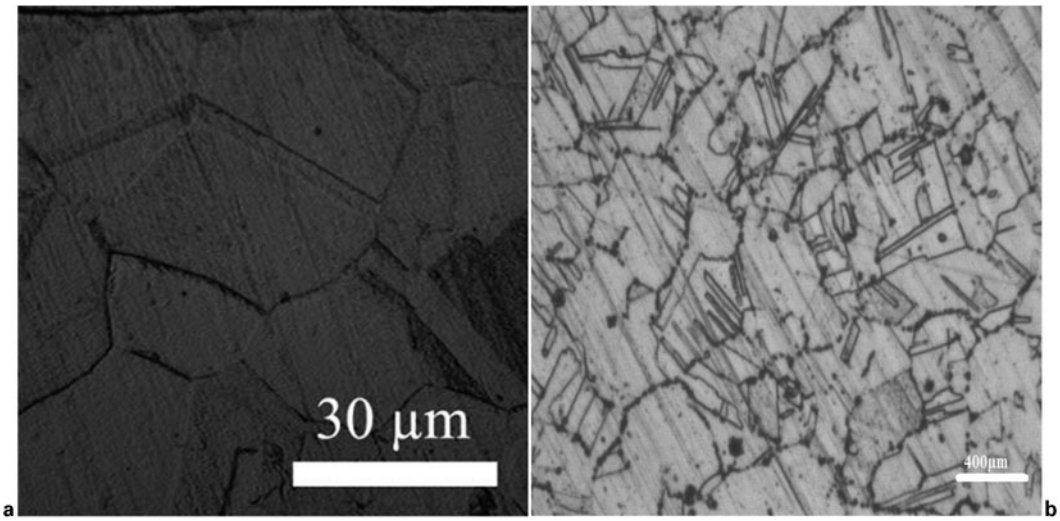

4 *a* SEM image and *b* photography of AISI 316L SS with acidic etchant (1 part HF, 2 parts HNO_3 and 3 parts H_2O)

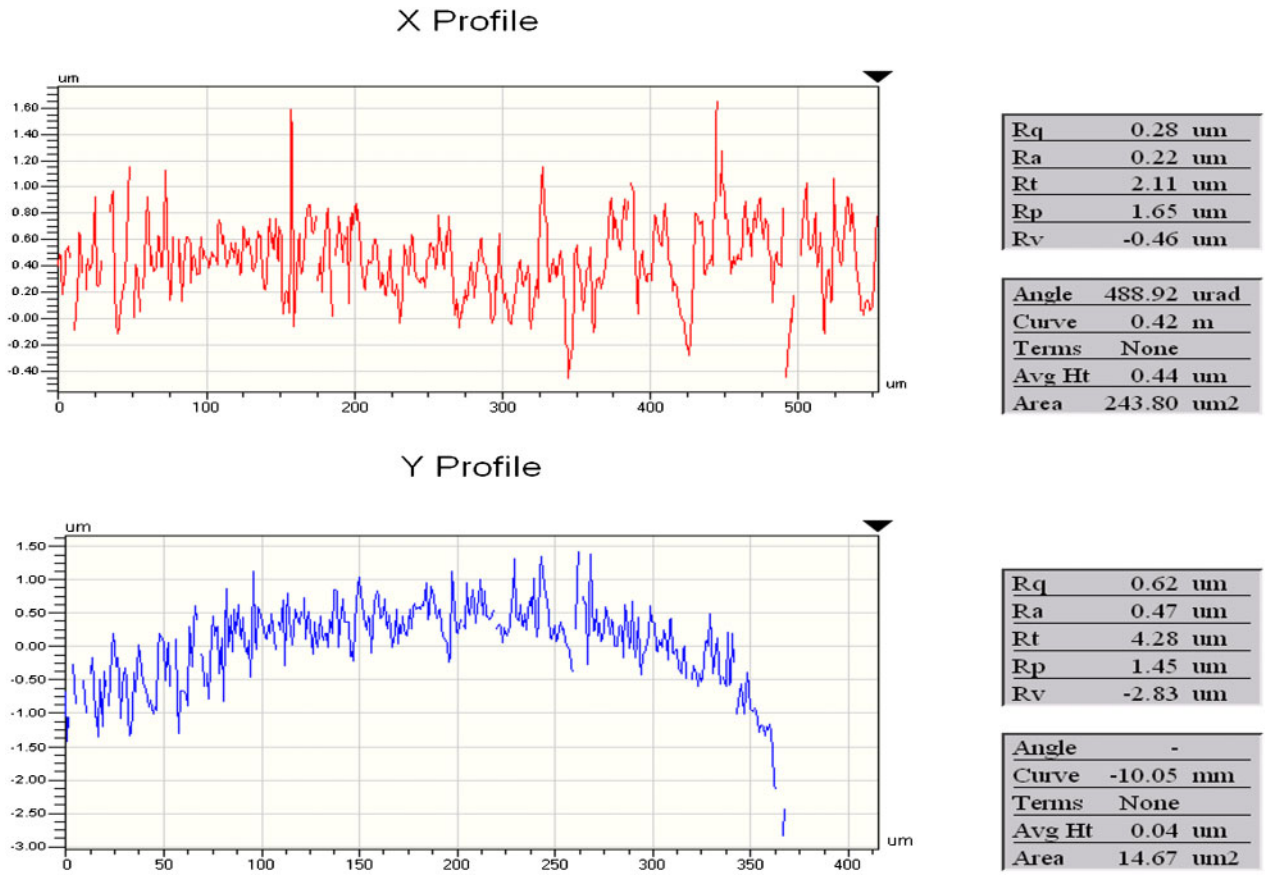

5 Optical two-dimensional trace of SS AISI 316L before wear test

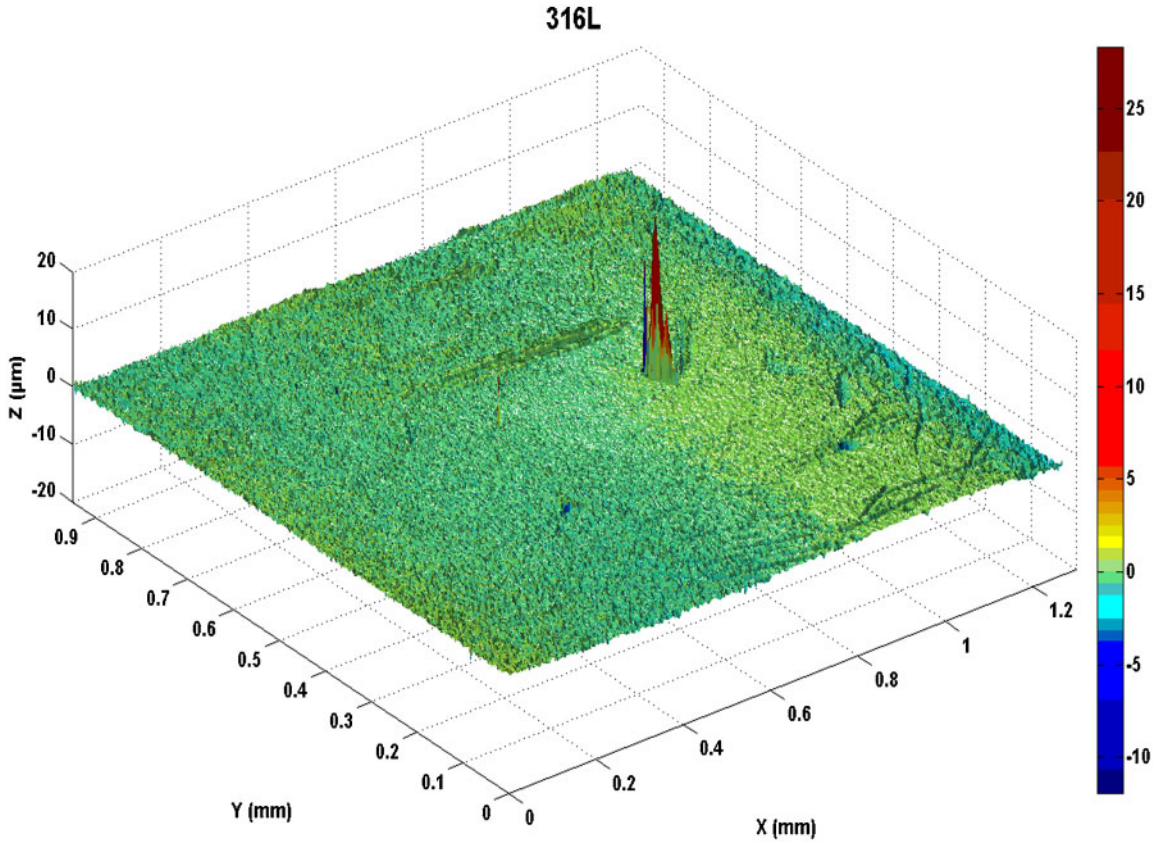

6 Optical three-dimensional photo of SS AISI 316L before wear test

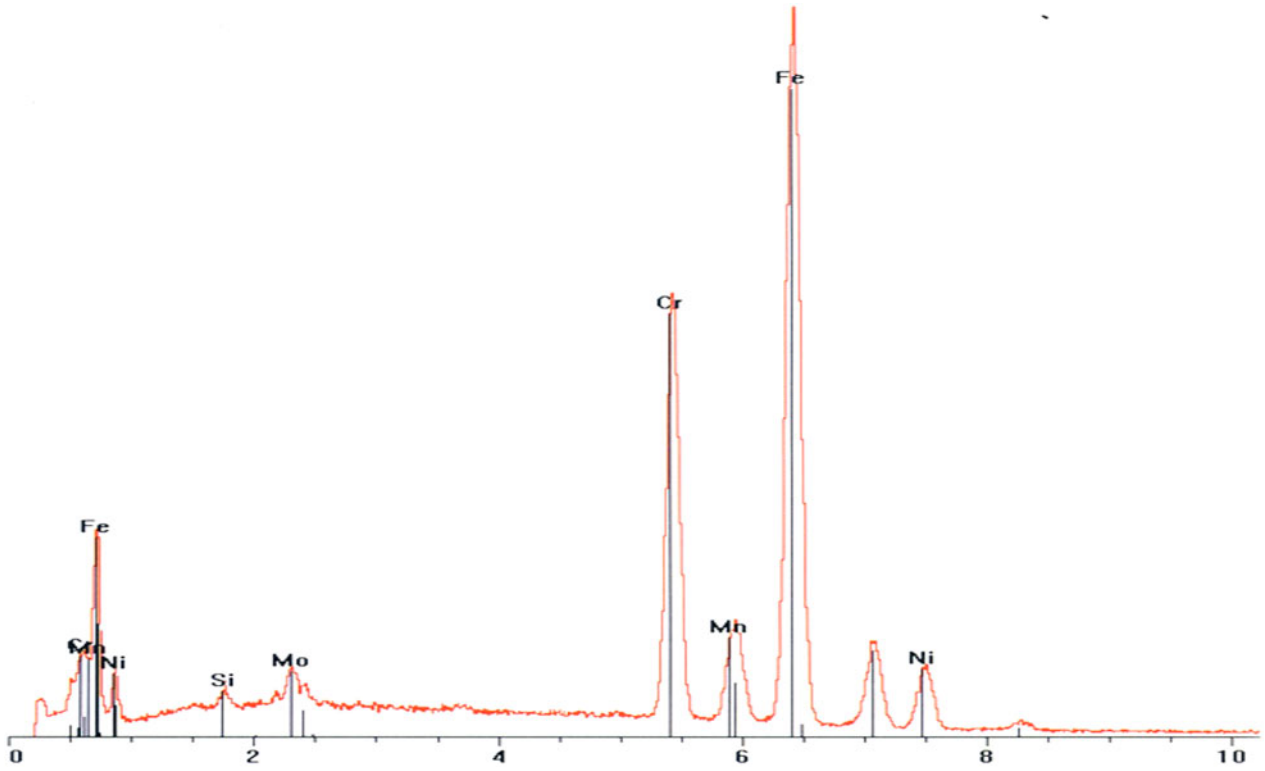

7 Energy dispersive X-ray analysis spectrum of SS AISI 316L

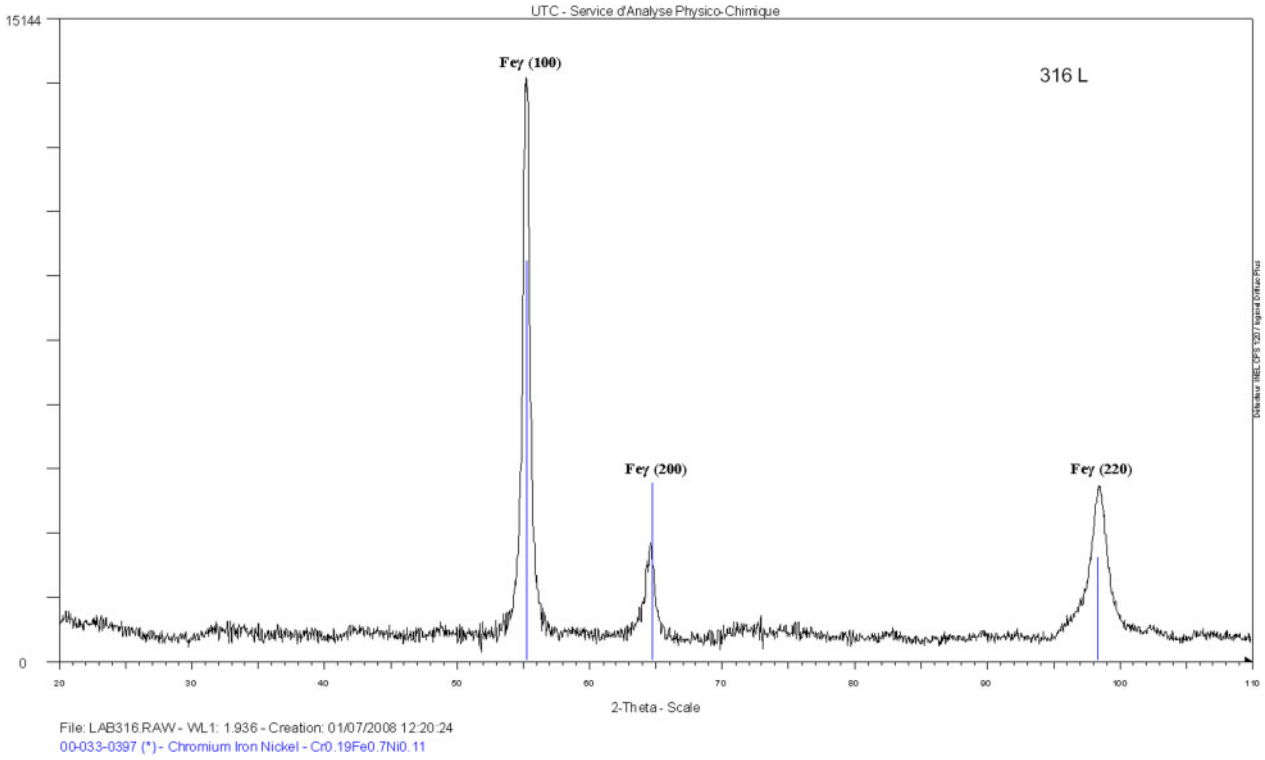

8 X-ray diffractometry spectrum of SS AISI 316L

Table 2 Work condition of alternative movement wear test oscillating tribotester

Friction pairs used	Ball 100C6/AISI 316L
Sliding speed	1, 15 and 25 mm s^{-1}
Normal load (load applied)	3, 6 and 10 N
Wear track radius	10 mm
100C6 ball diameter	10 mm
Temperature	25°C
Humidity	38%

Table 3 Roughness parameters of SS AISI 316L before wear test

R_a/nm	268·36
R_q/nm	384·47
R_z/nm	18 670·01
R_t/nm	40 232·59

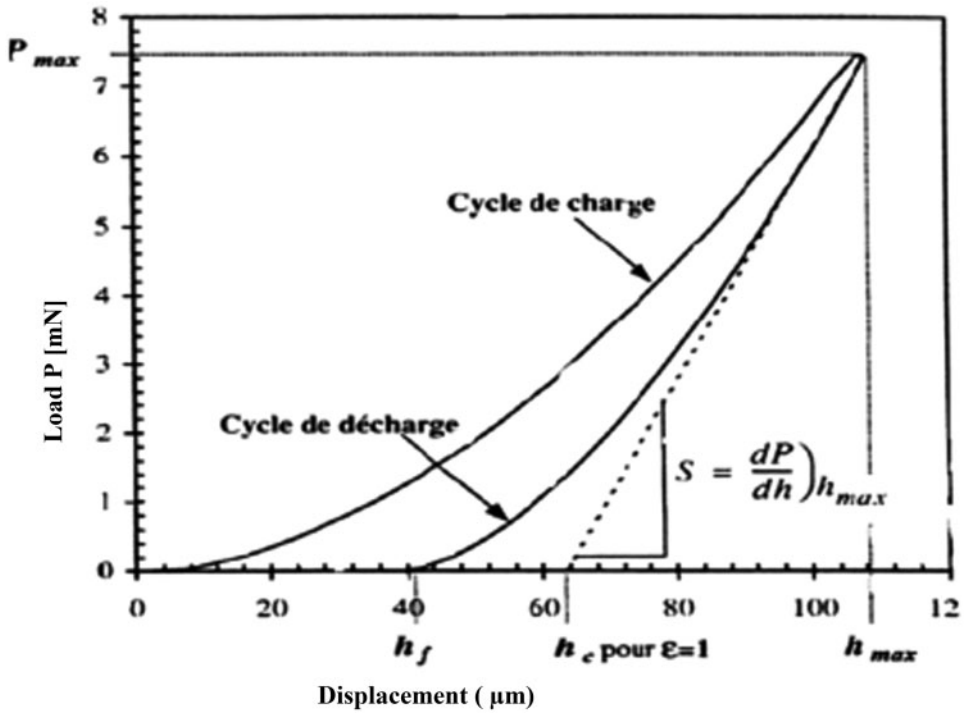

9 Example of microhardness curve[10]

and cause rashes or pain owing to release of nickel ions as evidenced from the above results.

The aim of this work is to evaluate and compare the tribological behaviour of the total hip prostheses used by SS AISI 316L (supplied by ENSAM Lille). The oscillating friction and wear tests have been carried out in ambient air with oscillating tribotester in accord with standards ISO 7148, ASTM G99-95a and ASTM G133-95. G the friction and wear tests were carried out to see the type of wear and to quantify the loss of mass. T the variation in the friction coefficient of the studied couples under different conditions of load (3, 6 and 10 N) and sliding speed (1, 15 and 25 mm s^{-1}) was also studied. As counter pairs, a 100Cr6 ball was used, 10 mm in diameter w. The results show that the weight loss quantifying the wear of a soft body slipping on a hard surface is proportional not only to the distance from the slip but also to the normal load applied.

The sliding speed has for a principal effect to act on the temperature of the contact zone. Going beyond a critical speed involves the surface fusion of the most fusible body.

The increase in the temperature of the contact with the speed induced to structure transformations increases the reactivity of surfaces with respect to the environment (oxidation in the presence of air). Above a certain temperature and thus for speeds of slip higher than a breaking value, the oxide film, resulting from a permanent oxidation, is reconstituted with the fur as it is destroyed by wear.

The behaviour observed in both samples under different conditions suggests that the wear mechanism during the test is the same, and to increase the wear and friction resistance of biomedical SS AISI 316L used in total hip prosthesis (femoral stems), surface coating and surface treatment are necessary.

Acknowledgements

This work was realised in collaboration with the mechanical laboratory LML of ENSAM Lille, France. M. Fellah wishes to thank the Laboratory of Metallurgy, ARTS ET METIERS Paris Tech in ENSAM Lille, for kindly supplying the AISI 316L as a femoral stem. We are also grateful to the director of the laboratory, A. Iost, for using the SEM and tribotester facility.

References

1. A. Duran, A. Conde, A. Gomezcoeds, T. Dorado and C. Garcia: 'Sol–gel coatings for protection and bioactivation of metals used in orthopaedic devices', *J. Mater. Chem.*, 2004, **14**, 2282.
2. M. Vallet Regi, I. Izquierdo Barba and F. J. Gil: 'Localized corrosion of 316L stainless steel with SiO_2–CaO films obtained by means of sol–gel treatment', *J. Biomed. Mater. Res. A*, 2003, **67A**, (2), 674–678.
3. R. B. Tracana, J. Sousa and G. S. Carvalho: 'Mouse inflammatory response to stainless steel corrosion products', *J. Mater. Sci.: Mater. Med.*, 1994, **9–10**, 596–600.
4. S. Nagarajan and N. Rajendran: 'Surface characterization and electrochemical behavior of porous titanium dioxide coated 316L stainless steel for orthopaedic applications', *Appl. Surf. Sci.*, 2009, **7**, 3927–3932.
5. A. G. De: 'la résistance causée dans les machines', *Mémoire de l'Académie Royale*, 1699, **12**, 257–282.
6. M. Conradia and P. M. Schönb: 'Surface analysis of localized corrosion of austenitic 316L and duplex 2205 stainless steels in simulated body solutions', *Mater. Chem. Phys.*, 2011, **130**, 708–713.
7. S. M. Hosseinalipoura and A. Ershad-langroudib: 'Characterization of sol gel coated 316L stainless steel for biomedical applications', *Prog. Org. Coat.*, 2010, **67**, 371–374.
8. H. Paetzold and E. Ilinich: 'Determination of the dynamic friction coefficient of cartilage with different biomaterials', *J. Biomech.*, 2008, **41**, (S1), page S286 DOI: 10.1016/S0021–9290(08)70285–9. ISSN: 0021–9290.

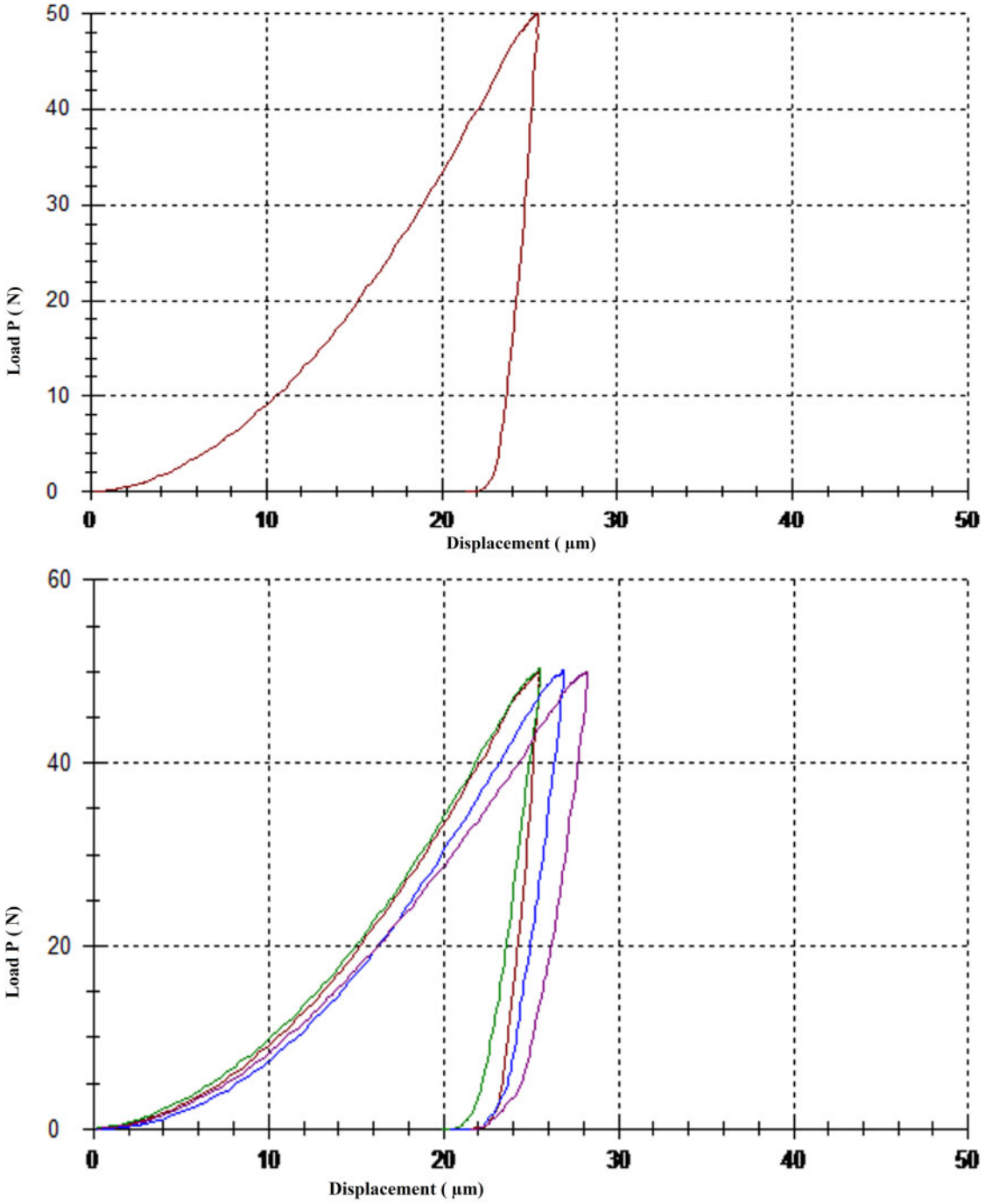

10 Microhardness curves of AISI 316L

9. E. Confortoa, B.-O. Aronssonb, A. Salitoc, C. Crestoud and D. Caillard: 'Rough surfaces of titanium and titanium alloys for implants and prostheses', *Mater. Sci. Eng. C*, 2004, **C24**, 611–618.
10. Norme Internationale (F): 'Implants chirurgicaux: Prothèses partielles et totales de l'articulation de la hanche – Partie 2: Surfaces articulaires constituées de matériaux métalliques, céramiques et plastiques', ISO 7206-2:1996.
11. L. Avril: 'Elaboration de revêtements sur acier inoxydable simulation de la fusion par irradiation laser caractérisation structurale, mécanique et tribologique', thèse, Ecole Nationale Superieure D'arts Et Metiers (no. d'ordre: 2003-16)
12. B. Tlili: 'Caractérisation de films durs multicouches élaborés par pulvérisation magnétron. Influence des conditions d'élaboration sur leurs propriété' le 9 décembre 2010 École doctorale no. 432: Sciences des Métiers de l'Ingénieur Doctorat ParisTech pastel-00573968, version 1–6 Mar 2011.
13. Z. Toughe, Z. Huixing: 'Comparative study of wear mechanism of surface treated AISI 316L stainless steel', *Surf. Coat. Technol.*, 2000, **128**, 1–8.

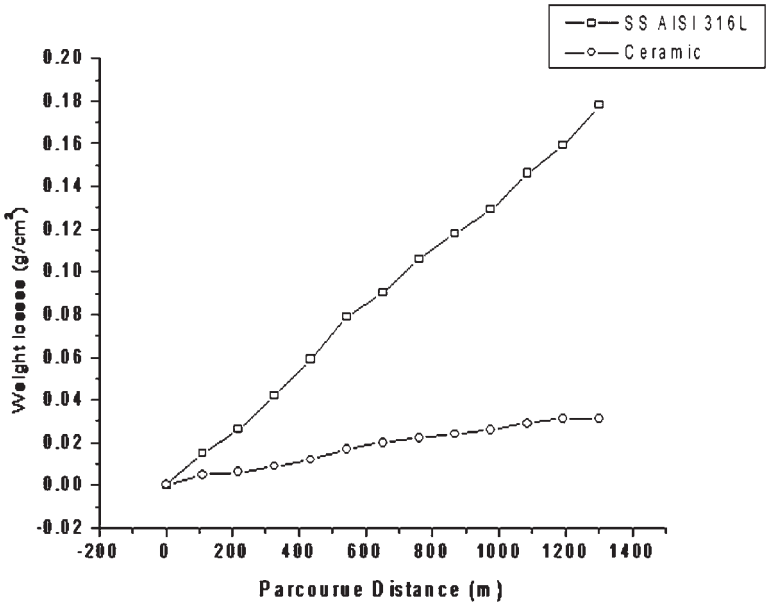

11 Wear diagrams (weight loss) of SS AISI 316L and ceramic sliding against (abrasive paper no. 320)

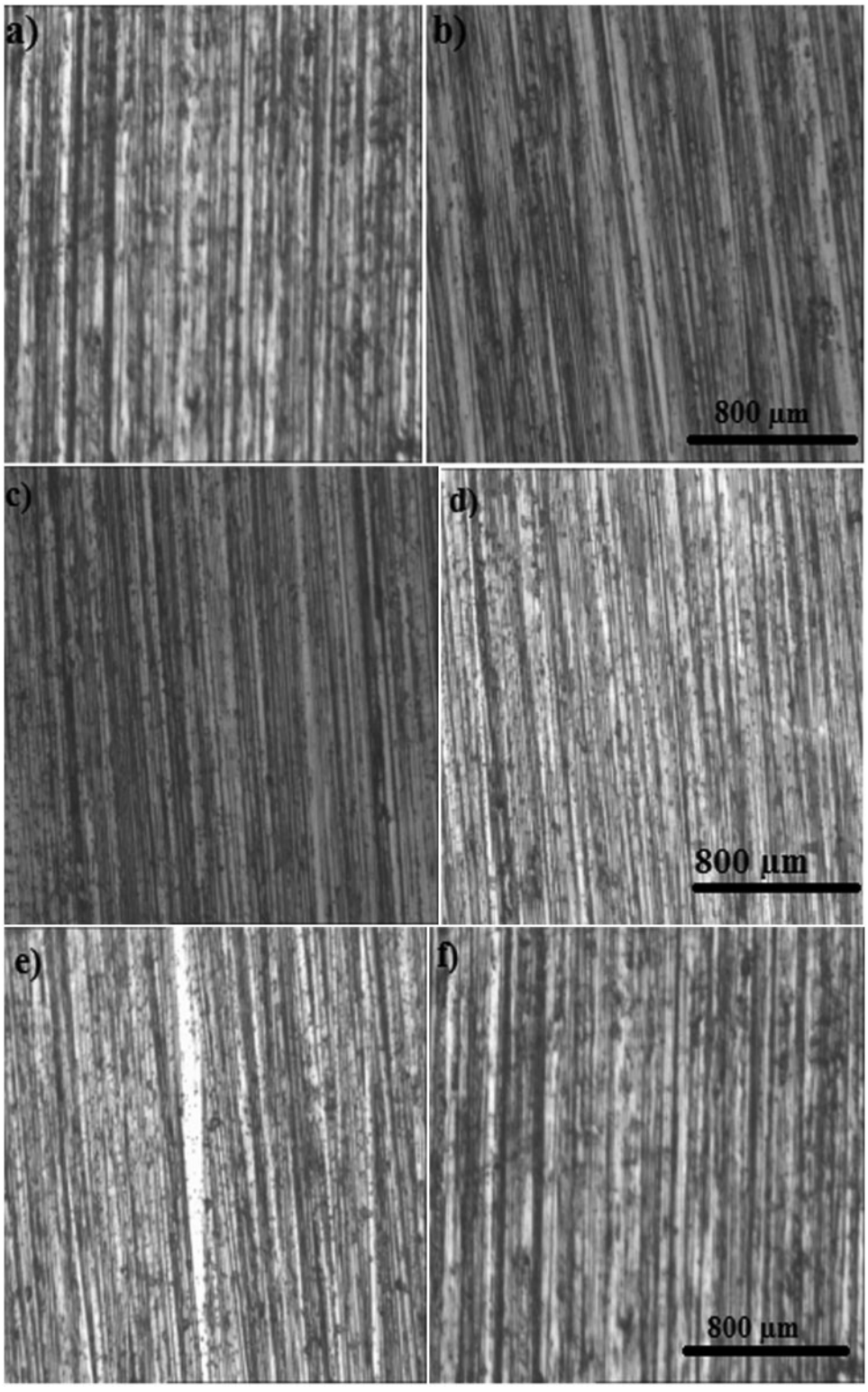

a 9 min; *b* 18 min; *c* 27 min; *d* 36 min; *e* 45 min; *f* 54 min

12 Morphology of SS AISI 316L surfaces tested against paper abrasive number 320 after different times: Gr × 50

Table 4 Mean coefficient of friction of SS AISI 316L versus times with different loads under tow sliding speeds of 600 and 1020 rev min^{-1}

Speed	1020 rev min^{-1}			600 rev min^{-1}		
Normal load *P*/N	19·43	28	43·95	19·43	28	43·95
Coefficient of friction	0·42	0·52	0·72	0·47	0·570	0·82

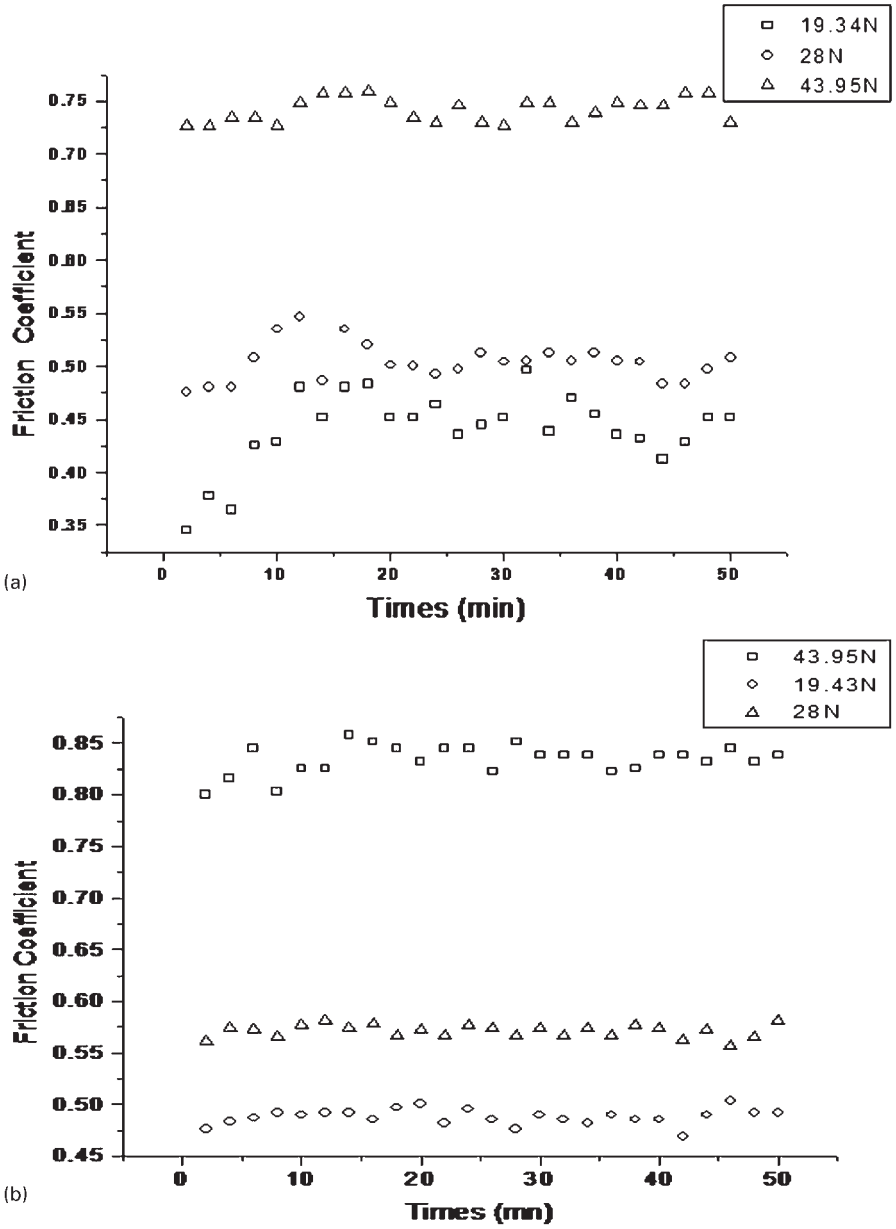

a 1020 rev min^{-1}; *b* 600 rev min^{-1}

13 Variation in friction coefficient versus times with different sliding speeds

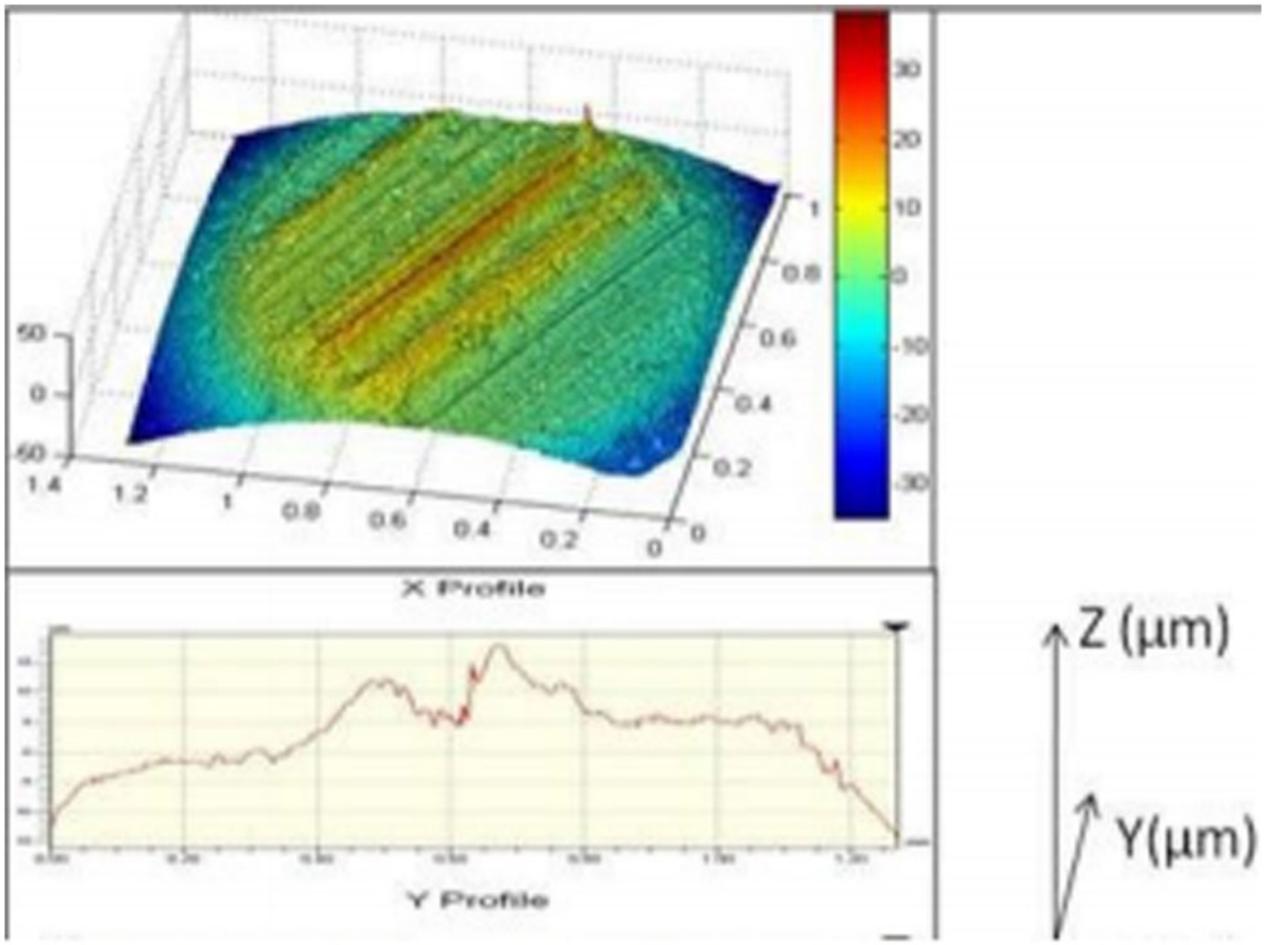

14 Wear marks of 100C6 steel ball under following conditions: t=1 h, FN=10 N, sliding speed=8 mm s^{-1} with same oscillating tribotester[10]

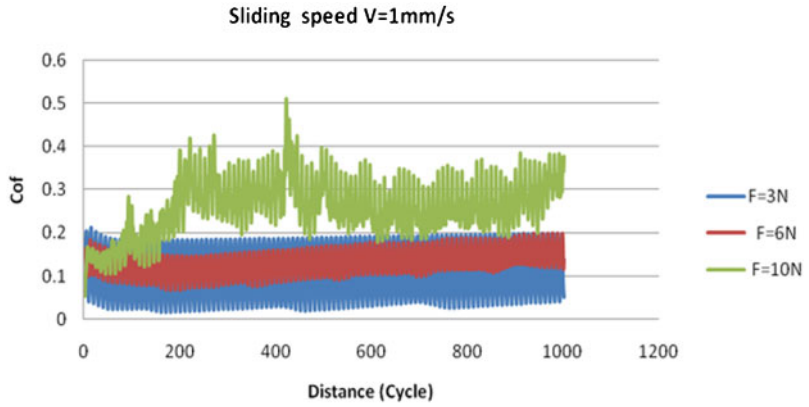

15 Friction test result of AISI 316l SS under sliding speed 1 mm s^{-1}

Table 5 Friction coefficient of SS AISI 316L versus different applied loads (3, 6 and 10 N) under sliding speed of 1 mm s^{-1} (after running in distance)

Sliding speed	1 mm s^{-1}				
Load/N	CF start	CF min.	CF max.	Mean CF	Hertz pressure/MPa
3	0·175	0·017	0·212	0·112	654
6	0·163	0·069	0·198	0·128	822
10	0·103	0·103	0·508	0·258	975

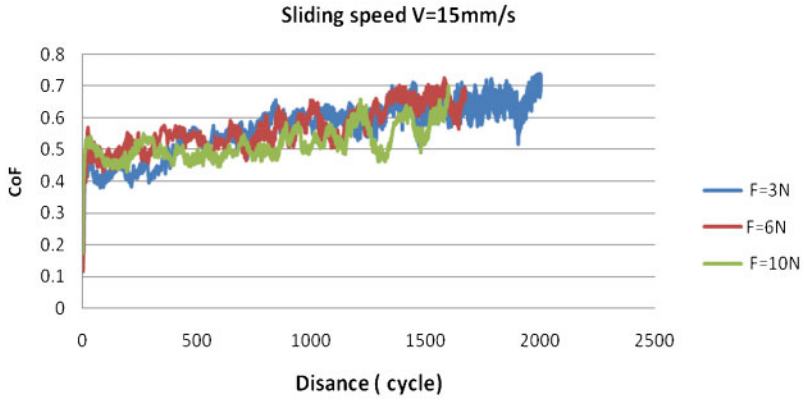

16 Friction test result of AISI 316l SS under sliding speed 15 mm s^{-1}

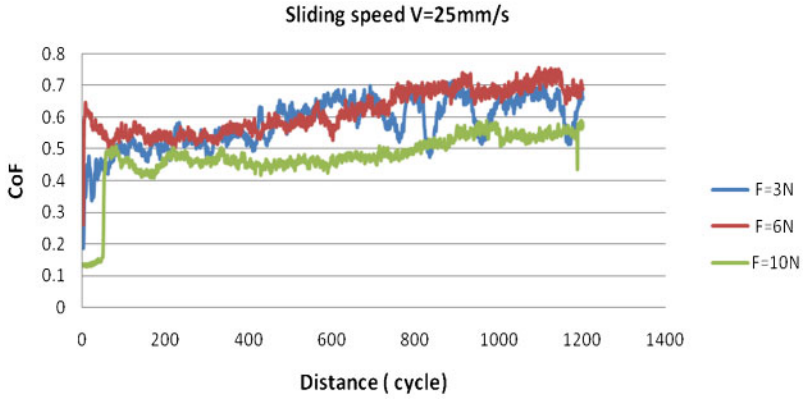

17 Friction test result of AISI 316l SS under sliding speed 25 mm s^{-1}

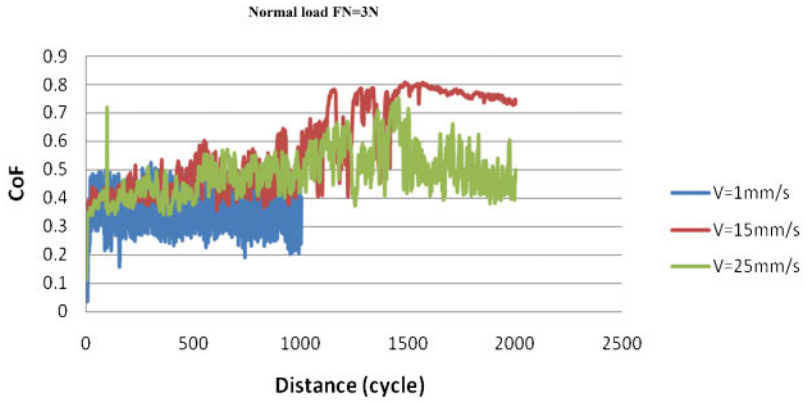

18 Friction test result of AISI 316l SS under normal load *FN*=3 N

Table 6 Friction coefficient of SS AISI 316L versus different applied loads (3, 6 and 10 N) under sliding speed of 15 mm s^{-1} (after running in distance)

Sliding speed		15 mm s^{-1}			
Load/N	CF start	CF min.	CF max.	Mean CF	Hertz pressure/MPa
3	0·195	0·17	0·74	0·568	690
6	0·124	0·124	0·726	0·566	870
10	0·263	0·263	0·7	0·519	1031

Table 7 Friction coefficient of SS AISI 316L versus different applied loads (3, 6 and 10 N) under sliding speed of 25 mm s^{-1} (after running in distance)

Sliding speed	25 mm s^{-1}				
Normal load/N	CF start	CF min.	CF max.	Mean CF	Hertz pressure/MPa
3	0·235	0·235	0·715	0·582	690
6	0·505	0·493	0·755	0·617	870
10	0·136	0·127	0·59	0·476	1031

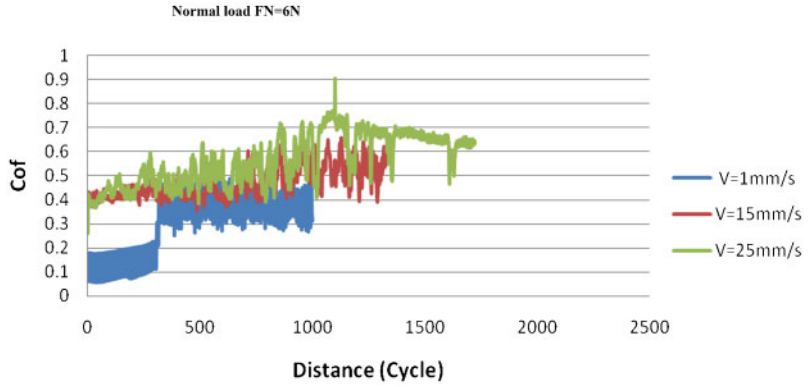

19 Friction test result of AISI 316l SS under normal load *FN*=6 N

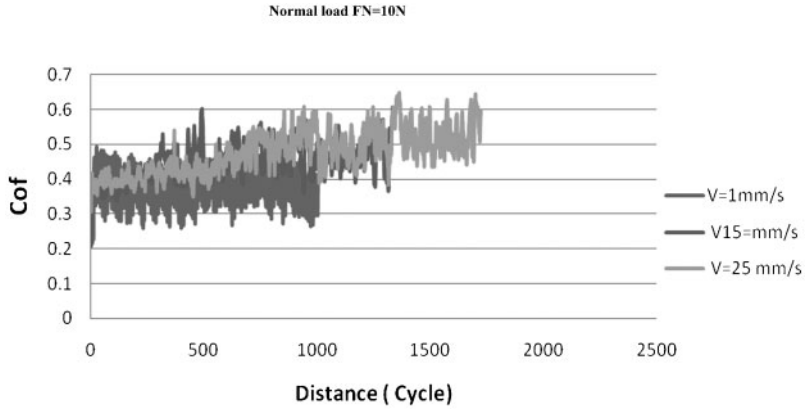

20 Friction test result of AISI 316l SS under normal load *FN*=10 N

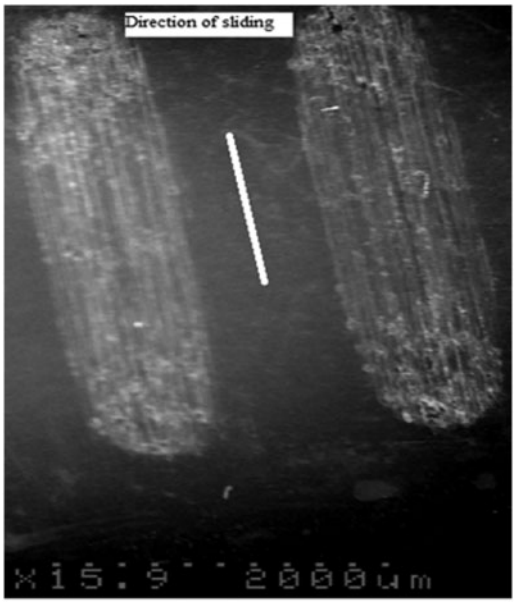

21 Wear tracks of AISI 316L SS

Table 8 Volumetric wear rate of AISI 316L under different conditions of applied load and speed

Sliding speed/mm s^{-1}	Load/N	Volumetric wear/mm^3 N^{-1} mm^{-1}
1	3	$7{\cdot}23 \times 10^{-3}$
	6	$9{\cdot}56 \times 10^{-3}$
	10	$15{\cdot}05 \times 10^{-3}$
15	3	$23{\cdot}67 \times 10^{-3}$
	6	$57{\cdot}1 \times 10^{-3}$
	10	$61{\cdot}5 \times 10^{-3}$
25	3	30×10^{-3}
	6	62×10^{-3}
	10	64×10^{-3}

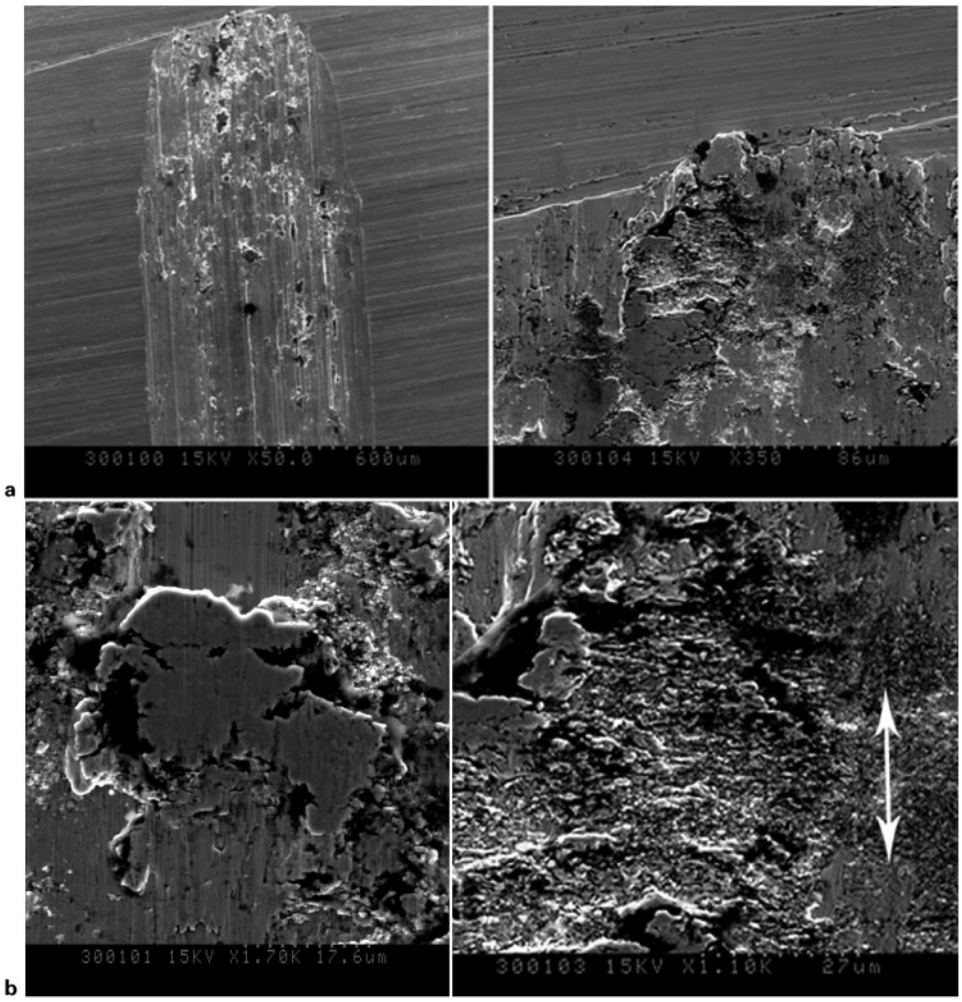

22 Photos of circular wear marks on 316L sample after friction test (severe deformation and plastic flow)